

**Advanced Characterization of Binuclear Azo Polymeric Resins for Enhanced Metal Ion
Uptake and Antibacterial Applications**

Dhivya Arumugam ^{1*}, Kaliyappan Thananjayan ²

¹Department of Chemistry, Puducherry Technological University, East Coasr Road, Pillaichavadi,
Pondicherry 605 014, India.

²Professor, Department of Chemistry, Puducherry Technological University, East Coasr Road,
Pillaichavadi, Pondicherry 605 014, India.

*Corresponding author: Dhivya Arumugam

E-mail: *dhivya654a@outlook.com*, tel: +91 91598 30828

ACCEPTED MANUSCRIPT

ABSTRACT

An acyclic dinuclear metal complex with O₄ donor coordination site was prepared and isolated. A polymethacrylate anchored coordination compound turned out to be designed by the combination of azo compound derived from 3-formyl salicylic acid and diazonium salt of 4-aminophenol with methacryloyl chloride and further polymerized using DMF solvent with benzoyl peroxide as initiator. The polychelates were isolated by treating the DMF solution of the resin with metal ions dissolved in water. The elemental analysis data strongly suggest 1:1 ligand-to-metal ratio, thus confirming the formation of a binuclear metal complex. The structure of the polymer and polychelates was confirmed by IR spectral data and the result reveals that the coordination of divalent metal is through oxygen of the aldehyde group, carboxylate ion, and phenolic –OH which in turn act as the bridging group. The electronic spectrum and magnetic moment values were used to justify the square planar and distorted octahedral structure for Cu (II) and Ni (II) polychelates. The increase in the crystalline nature of polychelates was explained using an XRD study. In addition, the synthesized polymer was experimented with for metal uptake properties under different pH and electrolytes which find applications in wastewater treatment. Also, the polychelates were studied for anti-bacterial activities with various micro-organisms using the agar well diffusion method, and the results are discussed.

Keywords: Micro-organisms, chelating resin, acyclic compartmental ligand, metal sorption properties, benzoyl peroxide.

1. Introduction

Binuclear azo polymeric resins are a distinctive class of materials known for their structural complexity and multifunctional properties (Kharpan et al. 2024). These resins feature azo ($-N=N-$) groups, which are integral to their chemical functionality, combined with a binuclear structural framework that enhances their molecular stability and versatility (Vasile Scaeteanu, Badea and Olar 2024). The unique combination of azo groups and polymer backbones results in materials with exceptional thermal, chemical, and optical properties, making them highly desirable for a wide range of applications (Albaaj and Mohammed). These resins are particularly valued for their potential in areas such as dye-sensitized materials, catalysis, and advanced optical coatings (Abdelhamid et al. 2024). The synthesis of binuclear azo polymeric resins involves carefully controlled organic reactions to achieve precise molecular architecture and tunable properties (Hangan et al. 2024). The binuclear configuration allows for enhanced molecular interactions and stability, enabling these resins to withstand harsh environmental conditions (Shen and Wang 2024). Furthermore, the azo groups introduce functionality like reversible photoisomerization, allowing these materials to exhibit photochromic and thermochromic behaviors (Abd El-Lateef, Khalaf and Abdou). These properties are pivotal for applications (Usha et al. 2024) in smart materials, sensors, and photonic devices, where material response to external stimuli is critical (Madavarapu et al. 2024; Malar, and Kumar, 2018). In addition to their industrial applications, (Jasmine Gnana Malar et al. 2023) binuclear azo polymeric resins are gaining attention in sustainable material science (Elmorsy et al. 2021). The design of these resins with high thermal resistance and UV stability makes them ideal for durable coatings and advanced composites (Younes et al. 2023). Ongoing research is exploring their use in nanotechnology and energy storage, highlighting their potential as eco-friendly alternatives in cutting-edge technologies (Mohammed, El-Ghamry and Saber 2021).

The development of binuclear azo polymeric resins faces several challenges that hinder their widespread application and optimization (Dahlous et al. 2023). Despite their remarkable thermal, chemical, and optical properties, issues such as complex synthesis processes, limited scalability, and

inadequate understanding of structure-property relationships remain significant barriers (Dancila and Bosomoiu 2024). Additionally, achieving precise control over their molecular architecture to tailor specific functionalities, such as photoisomerization (Balan et al. 2023) and environmental stability, is a persistent challenge (Mourer, Regnoul-de-Vains and Duval 2023). Furthermore, the environmental impact of certain synthesis methods and the limited exploration of sustainable approaches add to the complexity (Kuznetsova et al. 2020). Addressing these problems is essential to fully unlock the potential of binuclear azo polymeric resins for advanced applications in smart materials, photonics, and sustainable technologies (Dahlous et al. 2023). Insufficient exploration of polymethacrylate-supported (Malar et al. 2020; Sivasankari, 2019) azo derivatives hinders their potential in wastewater treatment and antibacterial applications. Additionally, complex synthesis processes, scalability issues, and inadequate understanding of structure-property relationships restrict the development of advanced azo polymeric resins. The primary contribution of this research paper is mentioned as follows.

- The study introduces a novel polymethacrylate-supported azo derivative of 3-formylsalicylic acid, which acts as a tribasic tetradentate ligand with O4 donor sites.
- The research synthesizes binuclear Cu(II) and Ni(II) polychelates with enhanced stability and functionality, characterized by different methods of spectroscopy (IR, ¹H-NMR, ¹³C-NMR), XRD, and thermal analyses (DSC and TGA).
- The study evaluates the metal adsorption behavior of the resin under varying pH and electrolyte concentrations, showcasing its applicability in wastewater treatment. Additionally, the antibacterial activity of the synthesized polymer and polychelates against six microorganisms is demonstrated, indicating potential for use in antimicrobial coatings.
- The research emphasizes the resin's high restoration capability (over 95%), ensuring its reusability without compromising sorption properties, thus supporting its practicality in real-world applications.

The remainder of this paper is arranged as follows: Section 2 summarizes the literature survey. Section 3 designates the comprehensive description of the proposed approach, and the result and discussion of the proposed method are covered in Section 4. Section 5 provides the conclusion and recommendations for further work.

2. Literature Survey

In this section, researchers have recently introduced several innovative techniques for the creation and description of metal complexes using azo-based ligands, as well as their applications in fields such as antibacterial activity, wastewater treatment, and catalytic systems, which are investigated in detail in the following section.

In (Li et al. 2023) synthesized earth-based compounds by combining pyridithione (1-hydroxy-2-pyridinethione; PT) with cerium (Ce III), samarium (Sm III), and europium (Eu III). Numerous characterizations were carried out, including single-crystal X-ray investigation, which demonstrated these complexes' fascinating binuclear structure. These results highlight the rare-earth complexes' encouraging potential for use in marine antifouling.

In (Morsy and Ebrahium 2023) presented an azo-azomethine ligand with nitrogen-donating and oxygen-donating atoms was created. Thermal, elemental, and spectroscopic investigations were used to describe the structure of the azo-azomethine ligand and its metallic chelates together with molar conductivity, magnetic susceptibility, and mass spectrometry measurements.

In (Kyhoiesh and Al-Adilee 2022) proposed [2'-(6-methoxybenzothiazolyl) azo] ligand 2--3,5-dimethyl benzoic acid (6-MBTAMB), which is generated has been used to produce several new Ag(I), Pt(IV), and Au(III) metal complexes from 2-amino-6-methoxy benzothiazole. Compared to conventional antibacterial medications (novobiocin) and antifungal medications (cycloheximide), these Complexes work less well against fungus and more well against bacteria.

In (Elsayed et al. 2023) presented the 3rd goal of the sustainable development strategy: attaining optimal health and promoting wellbeing. The copper(I) complexes of two redox-active hydrazo ligands, PyCHD, or pyridin-4-ylcarbonohydrazonoyl-dicyanide and

phenylcarbonohydrazonoyldicyanide (PCHD), synthesized and studied. According to the total binding energy values, the molecular docking studies against the SARS-CoV-2 major protease (ID: 6 WTT) demonstrated encouraging activity. $\text{PCHD} > \text{PyCHD} > [\text{Cu}(\text{PCHD})_2]\text{ClO}_4 \cdot \text{H}_2\text{O} > [\text{Cu}(\text{PyCHD})_2]\text{ClO}_4 \cdot \text{H}_2\text{O}$.

In (Kumar 2024) devised Numerous physical and spectroscopic methods, including nuclear magnetic resonance, infrared, electronic absorption studies, and elemental analysis (^1H and ^{13}C), and mass spectrometry, were used to confirm the structural characteristics of the produced azo dyes. According to the data, every azo dye under study shown competent and triggered biological effectiveness against the examined tests.

In (Khalaf, Abd El-Lateef and Abdou 2024) Synthesized with high yields in ethanol-based solutions, these complexes demonstrate exceptional stability and non-hygroscopic properties, with melting points exceeding 300°C . The outcomes include enhanced stability and bioactivity of metal complexes compared with their ligands, as well as promising therapeutic potential revealed through molecular docking analyses.

In (Lal et al. 2024) presented developments in different MOFs for use in water remediation through the photocatalytic breakdown and adsorption of water pollutants. Additionally, covered is the use of MOFs for water pollution detection using a variety of methods, including surface-enhanced Raman spectroscopy, colorimetry, electrochemical, and luminescence. The primary factors influencing MOFs' extensive applicability and enormous potential for commercial usage are their high porosity and chemical tunability.

In (Mohammed et al. 2024) introduced the microbial activities of copper (II) complexes against bacteria such as *Pseudomonas aeruginosa* and methicillin-resistant *Staphylococcus aureus* (MRSA), which represent Gram-positive and Gram-negative pathogenic strains, as well as clinically significant fungal strains such as *Candida albicans*, *Candida glabrata*, and *Candida tropicalis*. The complexes' performance closely matched the in vitro experiments' reactivity sequence.

In (Terenti et al. 2024) presented a 3,4-dihydroxybenzylidenehydrazine is synthesized, and its characteristics as a polymerization dopamine analog are examined. The novel polymer's coating ability and reaction process are ascertained and contrasted with those of polydopamine using an oxidative polymerization procedure. NaIO₄ was used as an oxidation reagent during the polymerization operations, which were conducted in a methanol–water combination.

In (MOHAMMED 2024) presented a (E)-4-(4-(dimethylamino) benzylidenamino)-2isopropyl-5-methylphenol which has C₁₉H₂₄N₂O formula, and 2-isopropyl-5-methyl-4-((5-methylfuran-2-yl) methyleneamino) phenol compound which has C₁₆H₂₀N₂O formula, have been produced and examined using spectroscopic techniques (FT-IR, NMR, UV-Vis) and single crystal XRD. The single crystal XRD result has shown that C₁₆H₂₀N₂O ligand crystallizes in the monoclinic crystal system with unit cell characteristics and space group P2₁/c. a= 10.119(11), b= 10.165(6) and c= 14.838(14) Å, and the angle β= 99.22(4) °, and molecular formula C₁₆H₂₀N₂O.

In this above literature review, existing methods limited exploration of polymethacrylate-supported azo derivatives for metal uptake and antibacterial applications, despite their potential in wastewater treatment and bacterial resistance. To overcome these challenges, advanced polymethacrylate-based azo polymers developed with improved thermal stability, enhanced sorption efficiency, and superior antibacterial properties.

3. Experimental Procedure

3.1. Materials

In Salicylic acid, hexamethylenetetramine, 4-aminophenol, and benzoyl peroxide were received from Merck and sigma Aldrich was utilized as received with no further purification. 3-FSA acid was prepared and obtained according to the Duff and Bills method. The solvents used were double distilled by regular procedures preceding their use.

3.2. Preparation

3.2.1. Synthesis of 3-formyl-2-hydroxy-5-((4-hydroxyphenyl) diazenyl) benzoic acid[3F2H5-4HPDABA]:

3-FSA (1.66g, 0.01mol) was added to dissolve in 20mL of conc. HCl by giving heat and cooled to -5°C. p-aminophenol (1.09g, 0.01mol) in 10mL of conc. HCl was cooled to -5°C with constant stirring. To the later, sodium nitrite (0.69g, 0.01mol) in 10mL water was added slowly and allowed to stir for half an hour. After the color change had occurred, 3-FSA/HCl solution was added drop by drop, and stirring continued for another half an hour. After, the brown suspension was neutralized with sodium carbonate solution and precipitated brown solids were filtered and desiccated.

3.2.2. *Synthesis of 5-((4-(methacryloyloxy) phenyl) diazenyl)-3-formyl-2-hydroxybenzoic acid [5-4MPDA3F2HBA]*

3-FSA (1.66g, 0.01mol) was added to dissolve in 20mL of conc. HCl by giving heat and cooled to -5°C. p-aminophenol (1.09g, 0.01mol) in 10mL of conc. HCl was cooled to -5°C with constant stirring. To the later, sodium nitrite (0.69g, 0.01mol) in 10mL water was added slowly and allowed to stir for half an hour. After the color change had occurred, 3-FSA/HCl solution was added drop by drop, and stirring continued for another half an hour. After, the brown suspension was neutralized with sodium carbonate solution and precipitated brown solids were filtered and desiccated.

3.2.3. *Synthesis of 5-((4-(methacryloyloxy) phenyl) diazenyl)-3-formyl-2-hydroxybenzoic acid [5-4MPDA3F2HBA]*

(3F2H5-4HPDABA) (1.43g, 0.005mol), TEA (0.7mL, 0.005mol), and EMK (50mL) were taken in a two-necked flask, one connected to a stopper funnel and another to the nitrogen cylinder, and the solution was cooled to -5°C. To the mixture, methacryloyl chloride (1.25mmol) in 10mL EMK was added drop and the stirring continued for another 2 hours. The quaternary salt of ammonia separated was decanted and the solvent was evaporated to achieve the monomer.

3.2.4. *Synthesis of polymer [poly(5-4MPDA3F2HBA)]*

(5-4MPDA3F2HBA) (1g) in 30mL of DMF and benzoyl peroxide (0.5g) was taken and transferred to a typical polymerization tube and thermostat for 10 hours at 70°C. The solution was then cooled transferred to excess distilled water and refrigerated for 24 hours. The polymer separated and settled

down and was decanted, washed with ethanol, and purified with a DMF/methanol combination. For consistent weight, the pure polymer was vacuum-dehydrated.

3.2.5. Synthesis of polymeric resin [poly(5-4MPDA3F2HBA)-M(II)] where M = Cu (II), Ni (II)

Poly(5-4MPDA3F2HBA) (5mmol of repeat component) was dissolved in 20mL of DMF and kept under stirring at room temperature. To the polymer solution, aqueous solution of copper acetate (5mmol) was added slowly and the solution's pH was balanced using dilute ammonia before the equilibrium was obtained. After 2 hours of stirring, the later reaction mixture was digested over a water bath and set aside for 24 hours at 27°C. The Cu (II) complex precipitated out was filtered, rinsed using purified water and ethanol, and dehydrated in a vacuum at 60°C. A similar method was acquired for the synthesis of Ni (II) polychelate.

3.2.6. Estimation of metal adsorption at varying pH

The resin dissolved minimum amount of DMF was reacted with liquid solutions of Cu (II) and Ni (II) of recognized strength of the solution. The solution's pH was balanced toward the preferred value with 0.1M HCl and 0.1M NH₃ and the reaction mixture was perturbed for 24 hours. The polychelates formed were filtered and rinsed using distilled water and the filtrate together with the washings was isolated separately. The metal ion concentration of Cu (II) was determined by standard complexometric titration technique and Ni (II) was determined by dimethylglyoxime method. The Synthesis of macromonomer 5-((4-(methacryloyloxy) phenyl) diazenyl)-3-formyl-2-hydroxybenzoic acid is shown in the Figure 1.

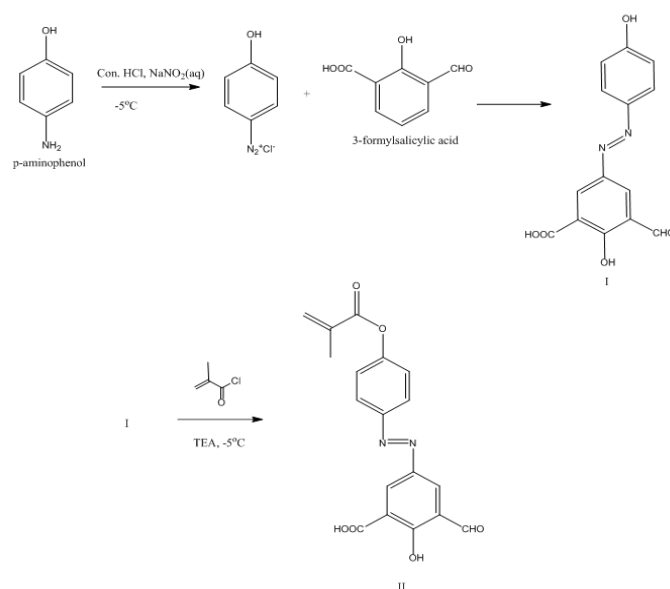


Figure 1. Synthesis of macromonomer 5-((4-(methacryloyloxy) phenyl) diazenyl)-3-formyl-2-hydroxybenzoic acid

3.2.7. Estimation of metal adsorption at various electrolyte concentrations

To 20mg of the resin dissolved in DMF, a known concentration of an electrolytic solution ($\text{NaCl}/\text{Na}_2\text{SO}_4$) was added. The solution's pH was maintained to the preferred value with 0.1M HCl and 0.1M NH_3 and the solution was kept under stirring for 24 hours at 27°C . To the aforementioned reaction mixture, 10mL of 0.1M aqueous solution of copper and nickel ions were transferred dropwise, and further stirring continued for another 24 hours. The poly chelates precipitated out were filtered, and rinsed with deionized water and the metal ion used up by the polymeric resin was examined by typical titrimetric procedure for Cu (II) and by dimethyl glyoxime procedure for Ni (II). The total metal ions used up against the resin were examined by the dissimilarity between a blank titration and the real titration results.

3.2.8. Preparation of microbial culture

Resistance to bacterial action of polymer resin and macromolecular azo polychelates was performed by the disc diffusion method. The name of the culture, sample, and standard are labeled at the bottom of the plate. Further, the agar-diffusion plate was nourished with bacterial strains and incubated for 24 hours. The test organisms used were *Bacillus subtilis*, *Candida albicans*, *Pseudomonas aeruginosa*, *Staphylococcus aureus*, *Staphylococcus epidermidis*, and *Escherichia coli*. A disc impregnated with

a known concentration of polymer resin and metal polychelates is positioned on the agar serving dish that was saturated culture of the bacterium to be tested across the entire plate. The antibacterial action of the polymer resin and macromolecular metal complex copper and nickel was tested with the listed microorganisms in dimethyl sulfoxide as the medium. The test concentration of $500\mu\text{g mL}^{-1}$ of the sample was used. For the diffusion of antimicrobial compounds into the agar, the plates were saturated at 50 degrees Fahrenheit for a day. The diameter of the inhibitory zone surrounding the disc determines the effectiveness of susceptibility. Organisms that grow to the disc's edge are resistant.

3.2.9. Restoration of polymer resin

The recovery of the polymer after chelation was tested using 25mL of 7molL^{-1} HCl. The metal polychelates remained positioned in the desorption average and agitated for 24 hours at ambient conditions. The metal ion proportion for desorption separated from the polymer-metal complex into the aqueous phase was examined by the number of metal ions originally used up by resin and the ultimate strength of divalent metal detached by the desorption medium. The Synthesis of poly[5-((4-(methacryloyloxy) phenyl) diazenyl)-3-formyl-2-hydroxybenzoic acid] metal complexes is shown in the Figure 2.

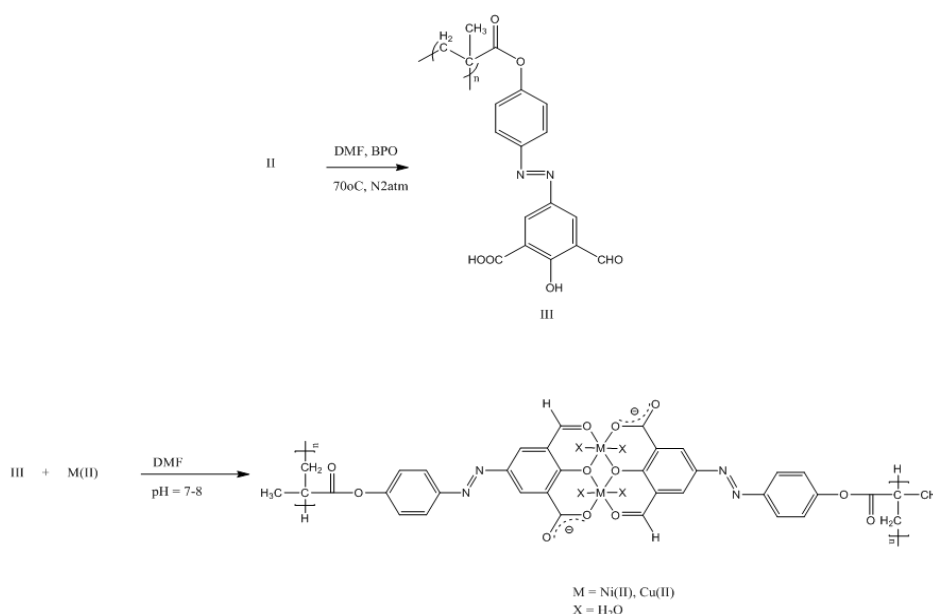


Figure 2. Synthesis of poly[5-((4-(methacryloyloxy) phenyl) diazenyl)-3-formyl-2-hydroxybenzoic acid] metal complexes

4. Results and Discussion

The Poly(5-4MPDA3F2HBA) was synthesized from Benzoic acid 3-formyl-2-hydroxy-5-((4-hydroxyphenyl) diazenyl) with methacryloyl chloride in the presence of hydroquinone with ethyl methyl ketone as solvent. The poly chelates of divalent metal ions were acquired from polymer dissolved in DMF solution and the divalent metal dissolved in aqueous solution in the presence of dilute ammonium solution. The prepared Poly(5-4MPDA3F2HBA) was solvable in DMSO, DMF, and chloroform but is not soluble in frequent organic solvents. The polymer-metal complex is only sparingly soluble in DMSO. All the polychelates are colored compounds. Table 1 shows the elemental analysis results for polymer and polychelates. All polychelates appear to have a 1:1 metal-to-polymer ratio based on elemental analysis data. Both the polychelates catalyze the reaction of ethyl acetate hydrolysis and also the initiation of polymerization of N-vinylbenzene.

Table 1. Elemental analysis for poly (APIMHB), and its metal complexes

Abbreviation	Elemental analysis (Wt%)									
Empirical formula	C		H		O		N		Me	
									tal	

		Calcd. a	Found	Calc d. ^a	Fou nd	Calcd. a	Found	Calc d. ^a	Fou nd	Cal cd. a	Fou nd
poly(5- 4MPD A3F2H BA)	C ₁₈ H ₁₅ O ₆ N ₂	60.84	60.86	4.25	4.26	27.04	27.05	7.88	7.90	-	-
poly(5- 4MPD A3F2H BA)- Cu (II)	(C ₃₆ H ₂₆ O ₁₂ N ₄) _x .Cu(II)	51.86	51.89	3.12	3.09	23.04	23.07	6.72	6.68	15.54	15.25
poly(5- 4MPD A3F2H BA)-Ni (II)	(C ₃₆ H ₂₆ O ₁₂ N ₄) _x .Ni(II)(H ₂ O) _y	48.24	48.26	3.80	3.79	28.59	28.61	6.25	6.23	13.11	13.13

Molecular weight measurements poly(5-4MPDA3F2HBA) has an inherent viscosity of 0.428 dL g⁻¹.

The resin's molecular weight was found to be reasonably high. The gel permeation chromatography was employed to ascertain the poly(5-4MPDA3F2HBA) molecular weights of $M_n = 1.63 \times 10^4$ and $M_w = 4.01 \times 10^4$, respectively. Index of polydispersity (M_w/M_n) of poly(5-4MPDA3F2HBA) were found to be 2.46. The results agreed by means of the viscosity value. The results strongly confirm the polymer chain is terminated by radical recombination.

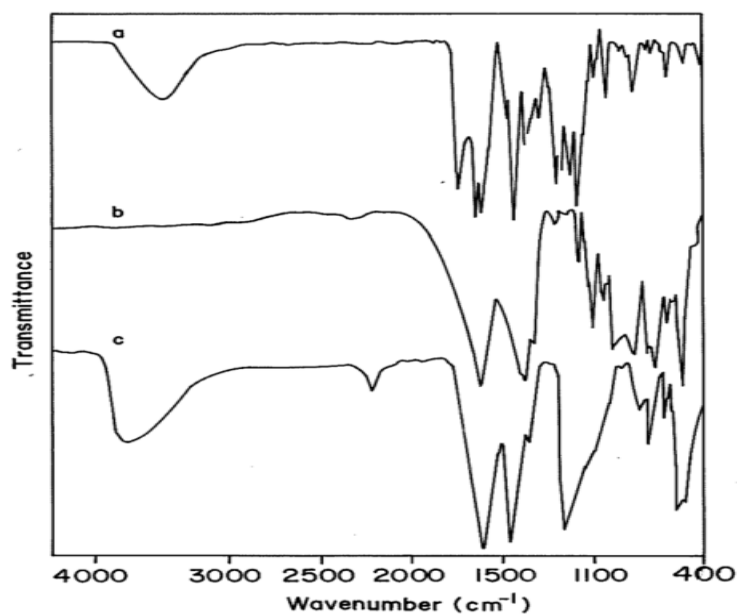


Figure 3. IR spectra of poly(5-4MPDA3F2HBA) (a), poly(5-4MPDA3F2HBA) Cu (II) (b) and poly(5-4MPDA3F2HBA) Ni (II) (c)

Spectral investigations of polymer and its metal complexes of the infra-red spectrum of Poly(5-4MPDA3F2HBA) as well as its Ni (II) and Cu (II) chelates are represented as indicated in Figure 3. The polymeric resin poly(5-4MPDA3F2HBA) shows a broad absorption in the range $3200\text{--}3700\text{cm}^{-1}$ which may be ascribed to --OH group stretching vibrations. This absorption is not found in the spectrum of polychelates confirming the contribution of --OH group to the participation of metal ion coordination. But in Ni (II) metal complex, there exist a broad absorption at 3900cm^{-1} , the value allocated for the phenolic --OH is the consequence of coordination of H_2O molecules to Ni (II) metal ion. This phenomenon was confirmed by heating up the Ni (II) polychelate to 150°C , even then the broad band did not disappear establishing the presence of water molecules. The stretching vibration of N=N is recorded in the region 1750cm^{-1} in the free polymer. The strong absorptions at $1620\text{--}1650\text{cm}^{-1}$ and $1480\text{--}1500\text{cm}^{-1}$ possibly be due to the C=O ester and acid groups. The average intense band at 1200cm^{-1} is responsible for the aromatic C-H system. The less intense peak at 2300cm^{-1} is designate to the C-H stretching of the aldehyde moiety. The vibration band at $400\text{--}500\text{cm}^{-1}$ and $600\text{--}700\text{cm}^{-1}$ reveals the construction of M-N and M-O bond correspondingly.

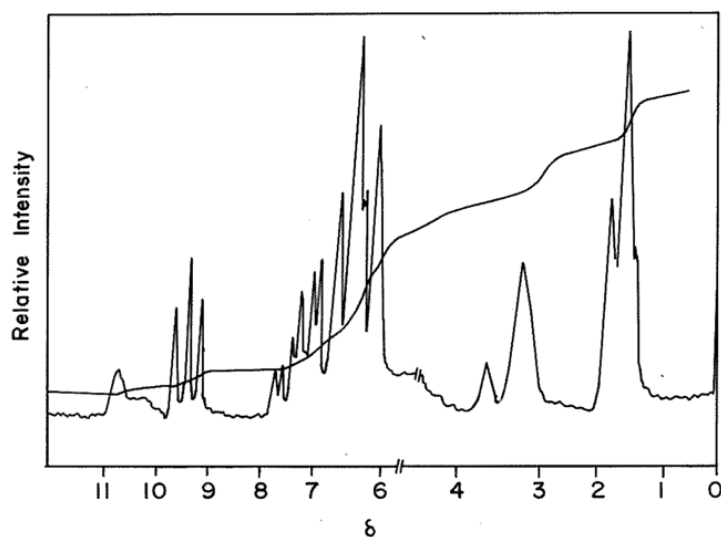


Figure 4. Proton NMR spectra of poly (5-4MPDA3F2HBA)

The proton NMR of poly(5-4MPDA3F2HBA) is represented in Figure 4. The wide multiplet in the area 7.9–6.2 δ are due to the resonance signals of aromatic hydrogen. The resonance signals in the region 2.5–1.2 δ are responsible for the methylene and methine protons. The resonance signal around 11 δ and 9 δ represents the carboxylic acid hydrogen aldehyde hydrogen. The sharp peak around 4-3 δ with a broad base indicates the phenolic –OH protons.

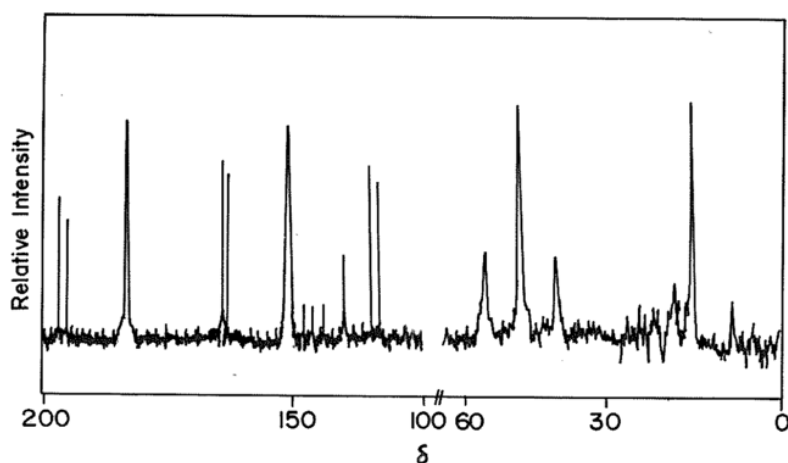


Figure 5. ^{13}C -NMR of poly(5-4MPDA3F2HBA)

The ^{13}C -NMR spectrum of poly(5-4MPDA3F2HBA) is represented in Figure 5. Peaks around 175–110 δ represent the aromatic carbon. The peaks in the region 185–170 δ represent the carboxylic acid and ester carbons. The peak above 185 δ shows the presence of aldehyde carbon and the peaks below 30 δ indicates the presence of methylene carbons

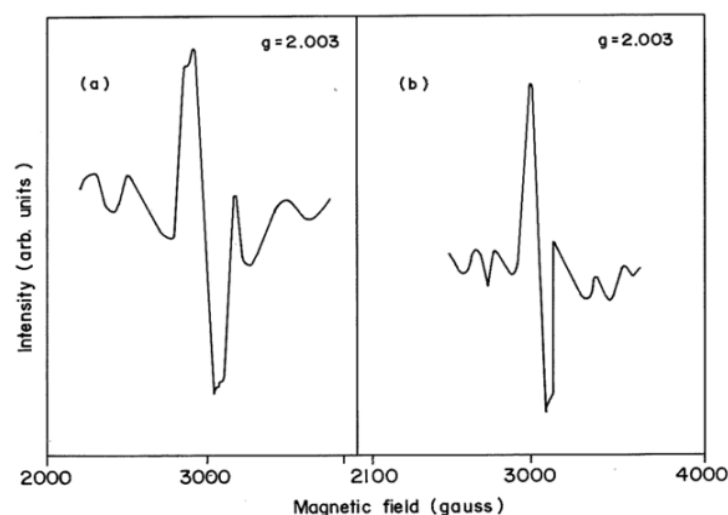


Figure 6. EPR spectrum of poly(5-4MPDA3F2HBA)-Cu (II) (a) and poly(5-4MPDA3F2HBA)-Ni (II) (b)

The EPR spectrum of the polychelates is presented in Figure 6. The copper complex has a strong signal in the EPR spectrum which is distinctiveness for a bivalent copper, and hence presumably ascribed to the square planar geometrical array of cupric ions in the core, which is surrounded by phenolic, ketonic, and carboxylate oxygen. Ni (II) complex with an octahedral discipline with tetrahedral distortion is predicted to experience a parameter for the spin-orbit coupling of g value greater than zero and consequently $g_{\parallel} > g_{\perp}$. The Ni (II) complex EPR parameters have been determined to be $g_{\perp} = 2.12$ and $g_{\parallel} = 2.25$, respectively. The g values for Ni (II) in an octahedral circumstance are fairly constant. A magnetic moment of 2.01 BM indicates a square planar geometry for Cu (II) polychelates. The deformed octahedral geometry of Ni (II) polychelates is suggested by the 3.95 BM magnetic moment and the paramagnetic character of Ni (II) complexes.

The X-ray sketches of Poly(5-4MPDA3F2HBA) and its metal complexes are represented in Figure 7. The XRD spectrum of Poly(5-4MPDA3F2HBA) revealed that the polymeric ligand is unstructured, but its respective polymer-metal complex exhibits a numeral reflection plane which is suggestive of the enhance crystalline nature in the polymer-metal complex. It is also noted that the crystalline nature found in metal complexes is not because of the arrangement of the polymeric ligand after chelation, yet, the tie up of metal ions to the polymeric ligand may cause inter-chain cross-linking in between the chains of polymer, whereby additionally diminish the ordering quite to increase any such

ordering. The outward show of crystalline properties in the polymer-metal complex would be the result of the metallic compounds' inherent crystalline nature.

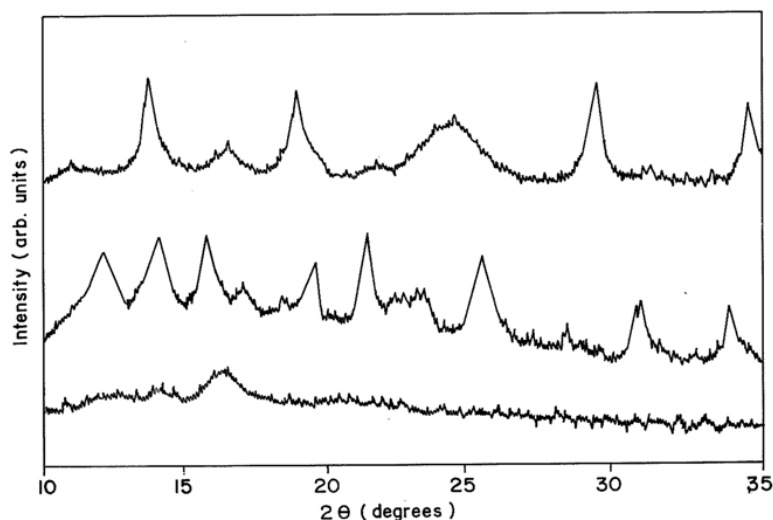


Figure 7. X-ray diffractogram of poly(5-4MPDA3F2HBA) (a), poly(5-4MPDA3F2HBA)-Cu (II) (b) and poly(5-4MPDA3F2HBA)-Ni (II) (c)

Figure 8 shows a representative DSC heating curve for poly(5-4MPDA3F2HBA) and associated polychelates. The T_g of Poly(5-4MPDA3F2HBA), Poly(5-4MPDA3F2HBA) -Cu (II), and Poly(5-4MPDA3F2HBA) -Ni (II) chelates was marked down as 255, 565 and 360°C, correspondingly. The cross-linking during the complexation is the reason for the transition difference.

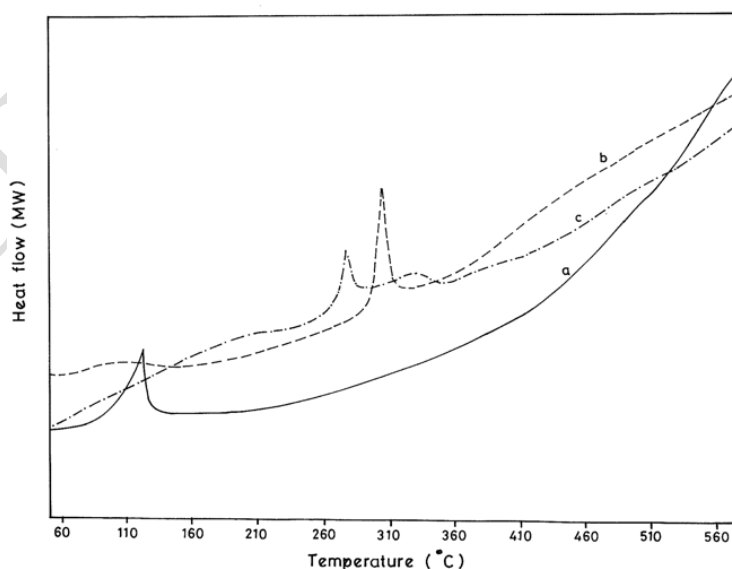


Figure 8. DSC heating curves of poly(5-4MPDA3F2HBA) (a), poly(5-4MPDA3F2HBA)-Cu (II) (b) and poly(5-4MPDA3F2HBA)-Ni (II) (c)

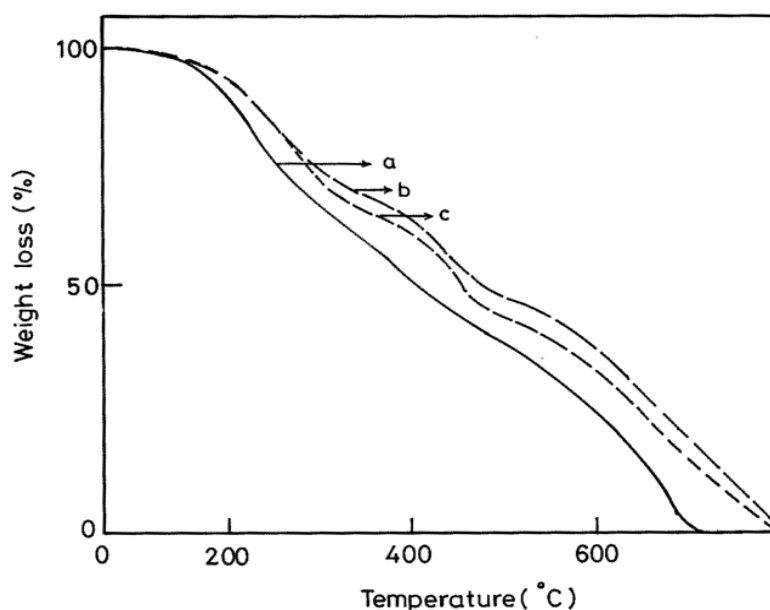


Figure 9. TGA traces of poly(5-4MPDA3F2HBA) (a), poly(5-4MPDA3F2HBA)-Cu (II) (b) and poly(5-4MPDA3F2HBA)-Ni (II) (c)

Thermograms of poly(5-4MPDA3F2HBA) and its macromolecular metal complex in the temperature region of 50-900°C are expressed in Figures 9, 10, 11, and 8% of the decomposition of polymer, Ni (II) and Cu (II) complex covering the region between 70-160°C corresponds to the water molecule or solvent captured by the resin. The loss of weight in the range of 180-450°C is because of the polymeric sequence degradation [almost 76% of polymer, 66% of Ni (II), and 54% of Cu (II)]. The metal oxide was the last degradation product in the case of polymer-metal complexes. This performance undoubtedly indicates that the polymeric azo derivative in the present research, which provides an O₃ donor site, exhibits a superior affinity for Cu (II) as opposed to that of Ni (II) metal ion; moreover, the involvement prohibited the split of hydroxyl and ketonic functional group. The divalent metal ions involved in the coordination of polymer chain cross-linking increase the thermal strength of the complex. The IR, ¹H-NMR, and XRD study long-established that coordination of the metal ions probably takes place involving two donor sites of different polymeric chains.

4.1. Application Study

4.1.1. Impact of pH on metal ion adsorption properties

The ionization and stability of the polymer and polychelates strongly depend on the pH variations. The consequence of pH on Cu (II) and Ni (II) metal ions uptake for Poly(5-4MPDA3F2HBA) against

aqueous solutions of divalent metal ions with an uptake time of 24 hours was carried out with varying pH. The results of metal ion adsorption at various pH differing from 2 to 10 are represented in Figure 10. In cooperation divalent metal ions experimented show the same behavior i.e. with an increasing pH the adsorption of metal ions increased. For Cu (II) polychelate, the precipitation of metal hydroxide takes place at pH above 7 and pH above 8 for Ni (II) polychelate which reveals the fact that the scope of metal ion uptake of Cu (II) is significantly high as compared to Ni (II).

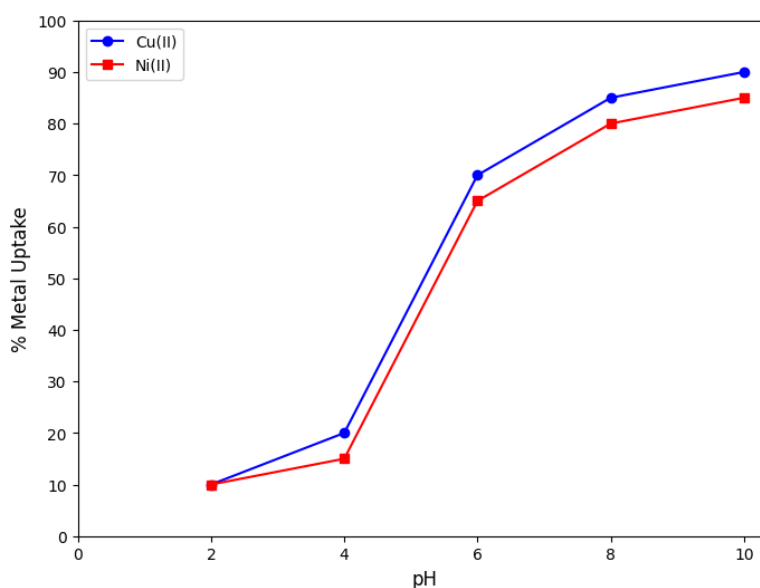


Figure 10. Polymer metal ion uptake behavior(5-4MPDA3F2HBA) resin at pH ranging from 2-10

4.1.2. Impact of electrolytes on metal ion adsorption properties

The total metal ion uptake with the known concentration of the resin and the electrolyte is represented in Table 2. In the attendance of electrolytes (i.e. Cl^- and SO_4^{2-} ions), the sorption property of Cu (II) and Ni (II) ions gradually raised in the company of escalating strength of the electrolytic solution. The above phenomenon probably be justified using the stability constant of the polychelates. The metal binding attraction of the resin in the presence of the electrolyte may be because of the scenery of the ligand in the replicate unit of polymeric resin.

Table 2. Poly Metal Uptake Percentage(5-4MPDA3F2HBA) with various electrolytes

Metal ion	pH	Electrolyte (mol L ⁻¹)	Percentage of the metal ion taken up in the presence of	
			NaCl	Na ₂ SO ₄
Cu (II)	3	0.01	19	19.6
		0.05	21.5	21
		0.10	23	23.7
	5	0.01	54	55
		0.05	56	57.4
		0.10	57.5	58
	7	0.01	83.5	84.5
		0.05	85	86
		0.10	87.3	87.5
Ni (II)	3	0.01	16	16.7
		0.05	17	18
		0.10	19.5	20.5
	5	0.01	53	52
		0.05	54.5	53.5
		0.10	57	57
	7	0.01	78	79.5
		0.05	79.5	80
		0.10	81	82.5

4.1.3. Resin restoration and reusability

Restoration referring to polymer from the Poly(5-4MPDA3F2HBA) complex were examined in a batch wise method. The polyclates were positioned in a desorption medium with 10mL of 7M HCl,

and total metal ions separated were experimentally calculated. The desorption ratio is, calculated using this equation.

$$\text{Desorption ratio} = \frac{\text{Amount of metal ions released}}{\text{Amount of metal ions adsorbed on resin}} \times 100$$

More than 95% of the polymeric resin was regenerated using a 7M HCl solution. The regenerated polymeric resin was used for polymer-metal complex formation and the regeneration of the metal ions was repeated three to four times as shown in Figure 11 to ensure the reusability of the polymer the results reveal the excellent reusability and steadiness of the polymer resin over acidic condition without any change in its sorption properties.

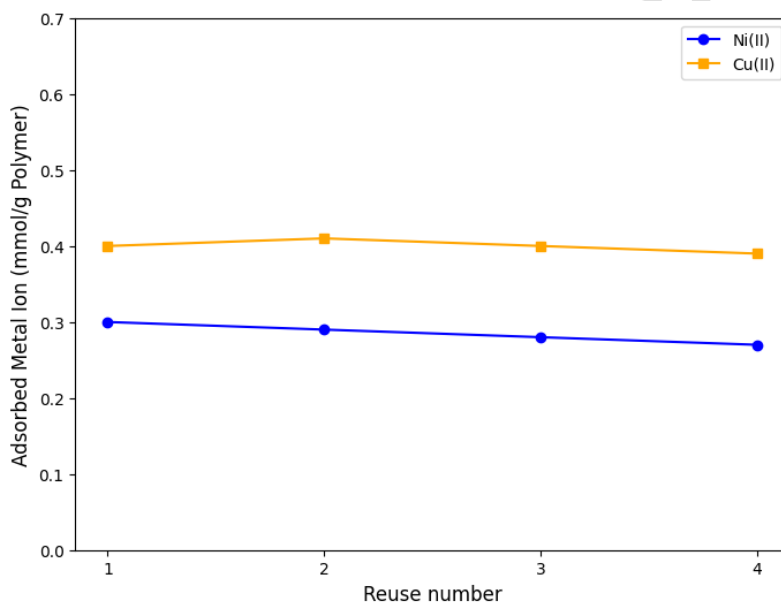


Figure 11. Regeneration of Poly(5-4MPDA3F2HBA) Cu (II) and Poly(5-4MPDA3F2HBA)-starting metal-ion concentration of 100 ppm, 0.02 g of polymer at a starting volume of 100 ml is used to adsorb pH 5 at 250C

Table 3. The antimicrobial properties of polymers and their metal complexes

Antibacterial disc assay (mm in diameter) zone of inhibition (mm) 100 µg disk ⁻¹							
Test Organisms							
S. no	Compound	Esherichi a coli	Basillus subtilis	Candid a	Pseudomon as aeruginosa	Staph ylococ	Staphyloco ccus

				albicans		cus aureus	epidermidis
1	Poly (5-4MPDA3F2H BA)	12	16	15	17	16	19
2	poly(5-4MPDA3F2H BA)-Cu (II)	17	19	16	20	20	22
3	poly(5-4MPDA3F2H BA)-Ni (II)	13	14	17	19	15	18
4	Kanamycin ^a	-	18	17	15	20	22
5	DMSO ^b	-	-	-	-	-	-

4.1.4. Antimicrobial activity

Table 3 reveals the results of microbial resistivity of the ligand and polychelates against experimented microorganisms. Both the ligand and the polymer-metal complex show a notable zone of inhibition and were compared to the standard drug of *kanamycin*(30mg). Compared to its parent ligand, the polychelate demonstrated superior antibacterial properties. Chelation reduces the core metal's polarity by partially sharing its positive charge with the electron-rich donor group. When this procedure is carried out, it makes the core metal ion more lipophilic, which aids in its entry into the membrane's lipid layer. The antibacterial action of the complexes was further enhanced by parameters likely magnetic moments, conductivity, stability constants, and also solubility.

Table 4: Comparative analysis of Existing models and Proposed model

Authors	Model	Key Features	Performance
---------	-------	--------------	-------------

Reddy et al., (2022)	Simple Azo Polymer- Metal Complex	Mononuclear coordination and Limited uptake	Cu uptake ~70% Antibacterial zone ~15 mm
Sharma and Gupta (2021)	Schiff base resin- metal complex	Moderate thermal stability, reusability not emphasized	Metal uptake <80% Moderate reusability
Khan et al., (2023)	Monomeric Azomethine Ligand Complex	Basic antibacterial screening and low Tg	Tg ~ 300°C, Low inhibition zones
Patel et al., (2020)	Polymer-supported transition metal complex	Poor regeneration and low surface interaction	Reusability <80%, Uptake <75%
Proposed	Binuclear Azo polymeric Resin	High uptake, strong antibacterial activity, admirable reusability and thermal stability	Cu uptake: 87.3%, Ni uptake: 81%, Tg: 565°C, ZOI: 22 mm, Reusability: >95%

Table 4 compares existing models of polymer-metal complexes with the proposed Binuclear Azo Polymeric Resin model. It compares several methods according to important features, uses, and performance indicators such thermal stability, metal uptake, reusability, and antibacterial activity. Schiff base resin-metal complexes with lower thermal stability and not emphasizing on reusability with metal uptake of less than 80%. Monomeric Azomethine Ligand Complex with the ability to possess basic antibacterial action but not exhibiting a significant glass transition temperature Tg value of ~300°C and pale inhibition zones. Polymer-supported transition metal complex having a poor regeneration value and lesser surface interaction with exhibiting reusability of less than 80% and metal uptake of less than 75%. The suggested Binuclear Azo Polymeric Resin exhibits high performance in all parameters. It exhibits excellent metal uptake (87.3% Cu and 81% Ni) and excellent antibacterial activity with a zone of inhibition (ZOI) of 22 mm. The proposed model also exhibits high thermal stability Tg: 565°C and it ideal for high-temperature applications.

5. Conclusion

In the current work, a new homo-binuclear Poly(5-4MPDA3F2HBA) was synthesized using a tridentate ligand and characterized. The ligand-to-metal ratio of 1:1 strongly suggests the formation of a binuclear metal complex. The thermal stability of the resin and poly chelates were found to be in the order poly(5-4MPDA3F2HBA)-Cu (II) > poly(5-4MPDA3F2HBA)-Ni (II) > poly(5-4MPDA3F2HBA). Poly(5-4MPDA3F2HBA) resin has a high divalent metal ions' capacity to bind over a wide pH range of 5-10. The polymer has elevated restoration capability with 95% devoid of any change in its sorption behavior. The results exposed that, the azo-based binuclear ligand can be successfully owned for the treatment of heavy metal ions from water and wastewater. Also, the antibacterial commotion of the polymer and polychelates can be used in bacterial-resistant coating materials. Future research focus on optimizing the synthesis process of binuclear azo resins to enhance their stability and environmental compatibility. Additionally, exploring their applications in diverse industries such as coatings and electronics will provide deeper insights into their practical potential.

Acknowledgements

The author would like to express his heartfelt gratitude to the supervisor for his guidance and unwavering support during this research for his guidance and support.

References

- Kharpan B., Pyngrope H., Bhattacharyya M., Shyam A., Wangkheimayum J., Pramanik H. A. and Mondal, P. (2024), Design amino acids Schiff base ligands and their Cu (II) and Zn (II) complexes as potent anticancer agent on human lung carcinoma, efficient CT-DNA binder, antibacterial and mesomorphic properties, *Journal of Molecular Structure*, 139075.
- Vasile Scaeteanu G., Badea M. and Olar R. (2024), Coordinative Compounds Based on Unsaturated Carboxylate with Versatile Biological Applications, *Molecules*, **29**(10), 2321.

- Albaaj L. T. T. and Mohammed M. Q. Schiff Bases and Their Polymer Resins in Aqueous Solutions: an Analytical and Adsorption Efficiency Study.
- Abdelhamid M. A., Khalifa H. O., Yoon H. J., Ki M. R. and Pack S. P. (2024), Microbial Immobilized Enzyme Biocatalysts for Multipollutant Mitigation: Harnessing Nature's Toolkit for Environmental Sustainability, *International Journal of Molecular Sciences*, **25**(16), 8616.
- Hangan A. C., Oprean L. S., Dican L., Procopciuc L. M., Sevastre B. and Lucaciu R. L. (2024), Metal-Based Drug–DNA Interactions and Analytical Determination Methods, *Molecules*, **29**(18), 4361.
- Shen C. and Wang Y. (2024). Recent Progress on Peroxidase Modification and Application. *Applied Biochemistry and Biotechnology*, 1-25.
- Abd El-Lateef H. M., Khalaf M. M. and Abdou A. Preparation, Characterization, In Vitro Biological Evaluation, DFT Calculations, and Molecular Docking Investigations of 1H-Imidazole-2-Carboxylic acid and Histidine-Based Mixed-Ligand Complexes, *Chemistry & Biodiversity*, e202402049.
- Usha, M., Mahalingam, T., Ahilan, A. and Sathiamoorthy, J. (2024). EOEEORFP: Eagle optimized energy efficient optimal route-finding protocol for secure data transmission in FANETs. *IETE Journal of Research*, **70**(5), pp.4867-4879.
- Madavarapu, J.B., Islam, H., Appathurai, A., Safdar, G.A., Muthukumaran, N. and Gnanamalar, J. (2024). Heterogeneous energy harvesting techniques for smart home IoT acceleration. *IEEE Access*.
- Malar, J.G. and Kumar, C.A. (2018). Implementation Of MPPT techniques for wind energy conversion system. *Int. J. Res. Anal. Rev.*, 5(3).

- Elmorsy E. E., Abdelghany A. M., Ayad D. M. and Gammal O. A. E. (2021), Synthesis and physicochemical studies of polyvinyl alcohol polymer modified with copper thiosemicarbazide complex, *Lett. Appl. NanoBioSci*, **10**, 2624-2636.
- Jasmine Gnana Malar, A., Ganga, M., Parimala, V. and Chellam, S. (2023). Estimation of Wind Energy Reliability Using Modeling and Simulation Method. In *International Conference on Frontiers of Intelligent Computing: Theory and Applications*. 473-480. Singapore: Springer Nature Singapore.
- Younes, A. A., Adam, A. M. A., Refat, M. S., Al-Wasidi, A. S., Almehizia, A. A., Al-Omar, M. A. and Asla, K. A. (2023), Synthesis of Bivalent Ni (II), Cu (II) and Zn (II) Complexes of Azodicarbonamide in Mixture of Methanol and Aqueous Solvents: Spectral Characterizations and Anti-Microbial Studies, *Crystals*, **13**(3), 367.
- Balan, S., Champla, D., Pushpavalli, M. and Ahilan, A. (2023). Energy Efficient Multi-hop routing scheme using Taylor based Gravitational Search Algorithm in Wireless Sensor Networks. *International journal of electrical and computer engineering systems*, *14*(3), 333-343.
- Mohammed, G. I., El-Ghamry, H. A. and Saber, A. L. (2021), Rapid, sensitive, and selective copper (II) determination using sensitive chromogenic azo dye based on sulfonamide, *Spectrochimica Acta Part A: Molecular and Biomolecular Spectroscopy*, **247**, 119103.
- Malar, A.J.G., Kumar, C.A. and Saravanan, A.G. (2020). Iot based sustainable wind green energy for smart cities using fuzzy logic based fractional order darwinian particle swarm optimization. *Measurement*, *166*, 108208.
- Dahlous, K. A., Soliman, S. M., Haukka, M., El-Faham, A. and Massoud, R. A. (2023), A New 1D Ni (II) Coordination Polymer of s-Triazine Type Ligand and Thiocyanate as Linker via Unexpected Hydrolysis of 2, 4-Bis (3, 5-dimethyl-1 H-pyrazol-1-yl)-6-methoxy-1, 3, 5-triazine, *Inorganics*, **11**(3), 135.

- Sivasankari, B., Ahilan, A., Gnana Malar A, J. and Ranjini V, S. (2019). Smart energy harvesting for intelligent railway condition monitoring system [articol].
- Dancila A. M. and Bosomoiu M. (2024), Exploring the Possibilities of Using Recovered Collagen for Contaminants Removal—A Sustainable Approach for Wastewater Treatment, *Polymers*, **16**(20), 2923.
- Mourer M., Regnouf-de-Vains J. B. and Duval R. E. (2023), Functionalized calixarenes as promising antibacterial drugs to face antimicrobial resistance, *Molecules*, **28**(19), 6954.
- Kuznetsova A., Matveevskaya V., Pavlov D., Yakunenko A. and Potapov A. (2020), Coordination polymers based on highly emissive ligands: Synthesis and functional properties, *Materials*, **13**(12), 2699.
- Dahlous K. A., Soliman S. M., Haukka M., El-Faham A. and Massoud R. A. (2023), A New 1D Ni (II) Coordination Polymer of s-Triazine Type Ligand and Thiocyanate as Linker via Unexpected Hydrolysis of 2, 4-Bis (3, 5-dimethyl-1 H-pyrazol-1-yl)-6-methoxy-1, 3, 5-triazine, *Inorganics*, **11**(3), 135.
- Li J., Zhu Q., Wu Y., Lin F., Liu L., Chen L. and Song L. (2023), Synthesis, Characterization, and Applications of Rare-Earth-Based Complexes with Antibacterial and Antialgal Properties, *ACS Applied Bio Materials*, **7**(1), 104-113.
- Morsy N. A. and Ebrahium M. M. (2023), Promoting the Antimicrobial Potency of Synthesized Azo-azomethine Triazole Ligand by Metal Complexing, *Egyptian Journal of Chemistry*, **66**(7), 297-317.
- Kyhoiesh H. A. K. and Al-Adilee K. J. (2022), Synthesis, spectral characterization and biological activities of Ag (I), Pt (IV) and Au (III) complexes with novel azo dye ligand (N, N, O) derived from 2-amino-6-methoxy benzothiazole, *Chemical Papers*, 1-34.

- Elsayed E. H., Al-Wahaib D., Ali A. E. D., Abd-El-Nabey B. A. and Elbadawy H. A. (2023), Synthesis, characterization, DNA binding interactions, DFT calculations, and Covid-19 molecular docking of novel bioactive copper (I) complexes developed via unexpected reduction of azo-hydrazo ligands, *BMC chemistry*, **17**(1), 159.
- Kumar V. (2024), Synthesis, Spectral Interpretation, and Biological Efficiency of Azo Colorants Derived from Sulfadiazine Moiety, *Polycyclic Aromatic Compounds*, **44**(3), 1835-1849.
- Khalaf M. M., Abd El-Lateef H. M. and Abdou A. (2024), Two Octahedral Ni (II) and Cu (II) Mixed-Ligand Complexes Incorporating 2, 6-Di (1H-Pyrazol-1-yl) Pyridine and 4, 4'-Bipyridine: Synthesis, Characterization, In Vitro Bioactivity, and Molecular Docking Exploration, *Applied Organometallic Chemistry*, e7897.
- Lal S., Singh P., Singhal A., Kumar S., Gahlot A. P. S., Gandhi N. and Kumari P. (2024), Advances in metal–organic frameworks for water remediation applications, *RSC advances*, **14**(5), 3413-3446.
- Mohammed T. P., Thennarasu A. S., Jothi R., Gowrishankar S., Velusamy M., Patra S. and Sankaralingam M. (2024), Investigation of the inherent characteristics of copper (II) Schiff base complexes as antimicrobial agents, *New Journal of Chemistry*.
- Terenti N., Fălămaș A., Bogdan D., Filip C., Vulcu A. and Petran A. (2024), Poly-3, 4-dihydroxybenzylidenhydrazine, a different analogue of polydopamine, *Nanotechnology Reviews*, **13**(1), 20240026.
- Mohammed S. A. (2024), *Investigation of X-Ray Single Crystal Structure And The Spectroscopic Properties Of Nitrogen Containing Aromatic Ring Compounds* (Doctoral dissertation).